PAPER

CrossMark
click for updates

A rapid and efficient ion-exchange chromatography for Lu–Hf, Sm–Nd, and Rb–Sr geochronology and the routine isotope analysis of sub-ng amounts of Hf by MC-ICP-MS†

R. Bast,[*a] E. E. Scherer,[a] P. Sprung,[b] M. Fischer-Gödde,[c] A. Stracke[a] and K. Mezger[d]

The development and improvement of MC-ICP-MS instruments have fueled the growth of Lu–Hf geochronology over the last two decades, but some limitations remain. Here, we present improvements in chemical separation and mass spectrometry that allow accurate and precise measurements of ^{176}Hf/^{177}Hf and ^{176}Lu/^{177}Hf in high-Lu/Hf samples (*e.g.*, garnet and apatite), as well as for samples containing sub-nanogram quantities of Hf. When such samples are spiked, correcting for the isobaric interference of ^{176}Lu on ^{176}Hf is not always possible if the separation of Lu and Hf is insufficient. To improve the purification of Hf, the high field strength elements (HFSE, including Hf) are first separated from the rare earth elements (REE, including Lu) on a first-stage cation column modified after Patchett and Tatsumoto (*Contrib. Mineral. Petrol.*, 1980, 75, 263–267). Hafnium is further purified on an Ln-Spec column adapted from the procedures of Münker *et al.* (*Geochem., Geophys., Geosyst.*, 2001, DOI: 10.1029/2001gc000183) and Wimpenny *et al.* (*Anal. Chem.*, 2013, 85, 11258–11264) typically resulting in Lu/Hf < 0.0001, Zr/Hf < 1, and Ti/Hf < 0.1. In addition, Sm–Nd and Rb–Sr separations can easily be added to the described two-stage ion-exchange procedure for Lu–Hf. The isotopic compositions are measured on a Thermo Scientific Neptune Plus MC-ICP-MS equipped with three 10^{12} Ω resistors. Multiple ^{176}Hf/^{177}Hf measurements of international reference rocks yield a precision of 5–20 ppm for solutions containing 40 ppb of Hf, and 50–180 ppm for 1 ppb solutions (=0.5 ng sample Hf 0.5 in ml). The routine analysis of sub-ng amounts of Hf will facilitate Lu–Hf dating of low-concentration samples.

Introduction

In addition to K–Ar, U–Pb, and Pb–Pb, the long-lived Lu–Hf, Sm–Nd, and Rb–Sr decay systems are among the most widely used chronometers for dating terrestrial rocks and meteorites. These systems often respond differently to heating and cooling, metamorphism, impact shock, or low-temperature alteration. Applying multiple chronometers to the same sample can therefore yield important information about its thermal history. In principle, many whole-rocks and minerals contain concentrations of trace elements that are sufficient to allow dating of <100 mg samples using multiple decay systems. In practice, however, it is often difficult to obtain enough pure mineral

separates for this purpose, especially when the sample size is limited as is the case for many meteorites. Angrites, for example, are not only rare meteorites (23 specimens altogether, mostly <1 kg total mass, of which only a few g are typically available for destructive analysis), but also contain Hf-poor minerals such as plagioclase (<20 ppb), olivine (<150 ppb), and phosphates (down to a few ppb). The latter two have relatively high Lu/Hf and are therefore important for increasing the range in ^{176}Lu/^{177}Hf among internal isochron points and precisely constraining dates.

Recent low-level Lu–Hf analyses (*e.g.*, Herwartz *et al.*,[4] Bast *et al.*[5]) have been performed following the chemical separation procedure of Münker *et al.*,[2] which is currently used—at least in part—by many laboratories. This method simplified the Lu–Hf separation from 3 or 4 column stages[1,6–9] to a single Ln-Spec column, greatly streamlining the chemical procedure for Lu–Hf work. During loading and initial rinsing, most major elements are not adsorbed onto Ln-Spec resin. Therefore, the elution profiles of Lu and Hf are not greatly affected by variable bulk sample compositions, and the Hf yield remains high even if large amounts (several grams) of sample are processed. A pre-separation of matrix elements by precipitation as described in

[a]*Institut für Mineralogie, Westfälische Wilhelms-Universität Münster, Corrensstr. 24, D-48149 Münster, Germany. E-mail: Rebecca.Bast@uni-muenster.de*

[b]*Institut für Geologie und Mineralogie, Universität zu Köln, Zülpicher Str. 49b, D-50674 Köln, Germany*

[c]*Institut für Planetologie, Westfälische Wilhelms-Universität Münster, Wilhelm-Klemm-Str. 10, D-48149 Münster, Germany*

[d]*Institut für Geologie, Universität Bern, Baltzerstraße 1+3, CH-3012 Bern, Switzerland*

This journal is © The Royal Society of Chemistry 2015

J. Anal. At. Spectrom., 2015, **30**, 2323–2333 | **2323**

earlier methods[6,8–10] is therefore unnecessary. Unfortunately, the single-column separation is not sufficient for high-Lu/Hf samples because the heavy rare earth elements (HREE) tail into the Hf fraction, leading to significant isobaric interferences on ^{176}Hf during MC-ICP-MS analysis. In addition, variable amounts of Zr and Ti may elute with Hf, depending on the exact molarity of the HCl–HF mixture used and perhaps also the condition or age of the Ln-Spec resin. The presence of these two elements in the Hf fraction can influence the mass bias behavior relative to that of Hf-only solution standards and thus compromise the accuracy of ^{176}Hf/^{177}Hf measurements.[2,8,11,12] As a workaround, Hf cuts can be passed through Ln-Spec resin twice for an improved separation[13] followed by an additional cation column to remove remaining HREE. Performing two passes through the Ln-Spec column has the additional advantage that a sample may be initially loaded without ascorbic acid,[13] which would otherwise elute with the Sm, Nd, Rb, and Sr-bearing matrix, complicating the later separation of these geochronologically important elements. Overall, the chemical separation for multiple radioisotope systems from a single sample aliquot is possible when using the method of Münker et al.[2] but requires the addition of at least 2 column stages, prolonging the procedure and increasing the analytical blank.

The purpose and goals of developing a new chemical separation method are to (1) decrease the amount of Lu in the Hf fraction to insignificant levels, (2) decrease the amount of acid required for efficient Ti elution, (3) improve the separation of Hf from Zr, (4) avoid ascorbic acid in eluted fractions that can be used for Rb, Sr, Sm, and Nd analyses, and (5) minimize the procedural blank. Each of these requirements will be explained in more detail below.

(1) Decreasing the amount of Lu (and Yb) in the Hf fraction

The isobaric interferences of ^{176}Lu and ^{176}Yb on ^{176}Hf are monitored by measuring the ^{175}Lu and ^{173}Yb signals during Hf isotope analysis. The Lu–Hf system is analogous to the ^{87}Rb–^{87}Sr system in that the radioactive parent nuclides (^{176}Lu, ^{87}Rb) are also the spike isotopes, and they isobarically interfere with their respective daughter isotopes (^{176}Hf, ^{87}Sr). It is therefore crucial to achieve complete parent-daughter separation before MC-ICP-MS analysis.

In the single-column procedure of Münker et al.,[2] Lu is eluted from the Ln-Spec resin before Hf, and—at least for some batches of Ln-Spec resin—residual Lu has been observed to tail into the Hf cut, especially for high-Lu/Hf samples such as garnet and apatite (Table 1). Lutetium in the Hf fraction of a spiked sample comprises not only a mixture of natural sample Lu and ^{176}Lu-enriched spike, but also any blank Lu accumulated *after* Lu elution, up to and including MC-ICP-MS sample introduction, *i.e.*, the Lu blank along the *Hf path* through the chemistry. Over this relatively long path (120 ml of acid used), the residual spiked sample Lu, which has the same ^{176}Lu/^{175}Lu as measured in the Lu isotope dilution (ID) measurement, gets continually diluted with blank Lu of natural composition as it is gradually

Table 1 Typical interference monitors observed during Hf isotope analyses in our laboratory for different chemical separation methods[a]

Fraction	n	Yb monitor (^{173}Yb/$^{176}\Sigma$)			Lu monitor (^{175}Lu/$^{176}\Sigma$)		
		Median	Min	Max	Median	Min	Max
3-stage anion exchange chromatography[7] with HF and H$_2$SO$_4$							
wr	8	0.00008	0.00007	0.0001	0.00005	0.00003	0.00009
Single-pass Ln-Spec[2]							
wr	59	0.0001	0.00003	0.007	0.0002	0.00005	0.008
grt	103	0.0004	0.00006	0.1	0.001	0.0001	0.09
ap	6	0.001	0.0007	0.003	0.001	0.0004	0.007
cpx	29	0.0001	0.00002	0.008	0.0002	0.00005	0.007
opx	11	0.0003	0.00001	0.01	0.0002	0.00007	0.02
plag	6	0.0001	0.00000	0.0006	0.0001	0.00003	0.0007
ol	3	0.01	0.007	0.02	0.01	0.008	0.02
Double-pass Ln-Spec[2,13]							
wr	10	0.000002	0.000001	0.00001	0.00003	0.00001	0.00009
Single-pass Ln-Spec[2], plus X12 cation column							
grt	19	0.00007	0.000008	0.001	0.0001	0.00005	0.0007
Double-pass Ln Spec, plus X12 cation column[33]							
wr	15	0.000003	0.00000	0.0004	0.00002	0.000007	0.001
grt	24	0.00006	0.00001	0.006	0.0002	0.00003	0.008
ap	4	0.00005	0.00000	0.0001	0.0001	0.00001	0.0002
lws	10	0.00002	0.00001	0.0002	0.00003	0.00001	0.0005

[a] Mineral abbreviations: wr: whole-rock, grt: garnet, ap: apatite, cpx: clinopyroxene, opx: orthopyroxene, plag: plagioclase, ol: olivine, lws: lawsonite. $^{176}\Sigma = {}^{176}$Yb + ^{176}Lu + ^{176}Hf. Hafnium fractions that yielded unacceptably high interference monitors (see text) had to be passed through an additional X12 cation column to remove HREE and re-analyzed before the ^{176}Hf/^{177}Hf data could be published.
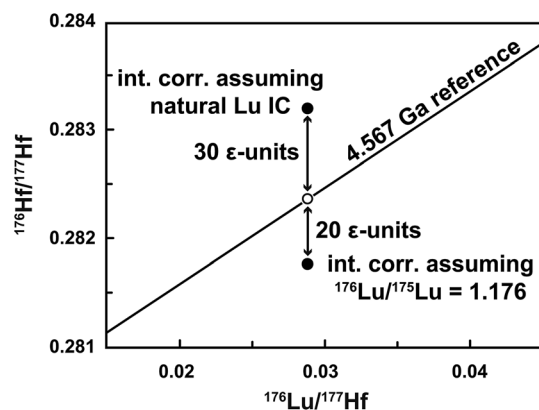
Fig. 1 Uncertainty related to the Lu interference correction on the $^{176}Hf/^{177}Hf$ of a spiked sample. In this example, the Hf isotope analysis of the plagioclase fraction from an angrite meteorite was affected by an extremely high Lu interference monitor ($^{175}Lu/^{176}\Sigma = 0.0042$). Using natural Lu ($^{176}Lu/^{175}Lu = 0.02656$) for the interference correction[8] results in a spuriously high $^{176}Hf/^{177}Hf$ value (undercorrection). Alternatively, assuming that the Lu has the same composition as that of the spiked sample ($^{176}Lu/^{175}Lu = 1.176$) results in an overcorrection and low $^{176}Hf/^{177}Hf$. The solar system reference isochron is based on the chondritic uniform reservoir (CHUR) parameters of Bouvier et al.[17] and the age of the solar system.[18] The open circle indicates the expected position of the plagioclase data point.

stripped from the column. The relative contributions of spiked sample Lu and the Hf-path Lu blank are highly variable and thus the $^{176}Lu/^{175}Lu$ of Lu in the Hf fraction is not easy to determine, leading to inaccurate interference corrections for spiked samples.

Isobaric interferences are typically corrected assuming natural isotope compositions (*e.g.*, $^{176}Lu/^{175}Lu = 0.02656$, $^{176}Yb/^{173}Yb = 0.7930$).[8,14] The subtraction of Yb can be done accurately,[12,15] whereas the amount of ^{176}Lu in the Hf fraction is often underestimated because the assumption of a natural Lu IC is not valid for samples spiked with a $^{176}Lu-^{180}Hf$ tracer. Simply using the $^{176}Lu/^{175}Lu$ of the spiked sample (measured during Lu ID analysis) for the interference correction[16] may, on the other hand, overcorrect $^{176}Hf/^{177}Hf$ to low values. This is shown in Fig. 1 for an isochron data point for which an extremely high Lu interference monitor ($^{175}Lu/^{176}\Sigma = 0.0042$, where $^{176}\Sigma = ^{176}Yb + ^{176}Lu + ^{176}Hf$, *i.e.*, the total signal measured at mass 176) was observed during the Hf isotope ratio measurement. The required interference correction was applied assuming either natural Lu (point above reference line) or the $^{176}Lu/^{175}Lu$ measured for the Lu ID analysis (point below reference line). The sample, a 60 mg angrite plagioclase separate (29 ppb Hf and 6 ppb Lu), was inadvertently over-spiked for both Lu ($^{176}Lu/^{175}Lu = 1.18$) and Hf ($^{180}Hf/^{177}Hf = 16.5$). In this extreme case, the ~50 ε-unit difference between the two end member corrections reveals a large uncertainty on the data point, which was consequently excluded from isochron calculations.

The effects of elevated Lu interference monitors are illustrated in Fig. 2. The error on $^{176}Hf/^{177}Hf$ arising from using a natural $^{176}Lu/^{175}Lu$ for the interference correction increases

with elevated $^{175}Lu/^{176}\Sigma$ especially for over-spiked samples, and can be calculated using the equation

$$\text{Maximum error in } \varepsilon\text{-units} = \left| \frac{\frac{^{176}\Sigma}{^{175}Lu} - \left(\frac{^{176}Lu}{^{175}Lu}\right)_{nat.}}{\frac{^{176}\Sigma}{^{175}Lu} - \left(\frac{^{176}Lu}{^{175}Lu}\right)_{ID}} - 1 \right| \times 10^4$$

where "nat." refers to the natural isotope composition of Lu and "ID" refers to the $^{176}Lu/^{175}Lu$ of the spiked sample. The green area in Fig. 2 represents properly spiked samples. For more strongly spiked samples, the error increases rapidly as a function of the Lu monitor. A $^{175}Lu/^{176}\Sigma$ of 0.0002, for example, adds an error of 1 ε-unit to the $^{176}Hf/^{177}Hf$ of a sample having a $^{176}Lu/^{175}Lu$ of 0.5, whereas the error remains close to measurement uncertainty for an optimally spiked sample.

Ideally, any Lu contamination of the Hf fraction should be avoided and the $^{175}Lu/^{176}\Sigma$ interference monitor should then be below 0.0001. To demonstrate high data quality, it would be useful to report the observed interference monitors with $^{176}Hf/^{177}Hf$ values that are used for isochrons. The $^{175}Lu/^{176}\Sigma$ monitor is preferred over *e.g.*, $^{175}Lu/^{177}Hf$, because the former is proportional to the applied interference correction in ε-units regardless of how radiogenic the samples are (*e.g.*, $^{176}Hf/^{177}Hf_{garnet} = 0.284$ *vs.* $^{176}Hf/^{177}Hf_{gadolinite} = 260$) and therefore allows direct comparison of interference effects on $^{176}Hf/^{177}Hf$ between non-radiogenic and extremely radiogenic samples.

A separation procedure that employs an initial cation column (*e.g.*, Patchett and Tatsumoto,[1] Wimpenny et al.,[3] Vervoort et al.,[14] Bizimis et al.[19]) is advantageous because the high field strength elements (HFSE) including Hf are not adsorbed onto the AG 50W-X8 cation resin whereas the REE are. Hence,
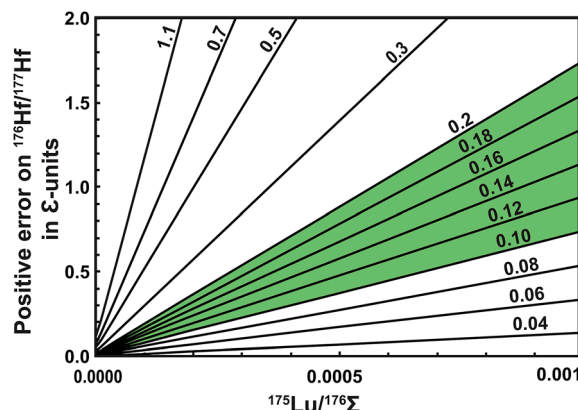

Fig. 2 Potential errors on $^{176}Hf/^{177}Hf$ stemming from elevated Lu interference monitors during Hf isotope analysis of spiked samples. Online interference corrections typically assume natural Lu composition ($^{176}Lu/^{175}Lu = 0.02656$),[8] and will thus not correct for the contribution of ^{176}Lu from the spike. The values for the sloping lines represent different $^{176}Lu/^{175}Lu$ of spiked samples; the green area shows the range of ideal spiking. These values are high enough to prevent unnecessary error magnification in Lu concentration, but low enough to avoid significant positive errors in $^{176}Hf/^{177}Hf$ at typical Lu-monitor values (*i.e.*, $^{175}Lu/^{176}\Sigma < 0.0001$).

This journal is © The Royal Society of Chemistry 2015

J. Anal. At. Spectrom., 2015, **30**, 2323–2333 | **2325**

the REE are eluted after Hf, which prevents tailing into the Hf fraction. However, care must be taken not to overload the column or breakthrough of the HREE might occur. The procedure outlined below adopts a miniaturized version of Patchett and Tatsumoto's[1] cation column. The isolation of Hf from the HFSE cut is performed on an Ln-Spec column devoted to this purpose, which never gets loaded with REE-bearing bulk samples, thereby eliminating potential Lu (+Yb) contamination.

(2) Optimization of the Ti elution

Blichert-Toft et al.,[8] Münker et al.[2] and Weyer et al.[11] have shown that the accuracy of the $^{176}Hf/^{177}Hf$ measurement by MC-ICP-MS is compromised by insufficient Ti removal. In the separation procedure of Münker et al.,[2] Ti is eluted as a peroxide complex with up to 50 ml of 0.45 M HNO$_3$—0.09 M citric acid—1 wt% H$_2$O$_2$. In other methods[1,3,7] Ti is complexed with H$_2$O$_2$ *before* loading the sample onto the column, which generally results in a more efficient elution of Ti and frees up resin capacity for the following separation of Zr from Hf. This is not feasible when loading in HCl,[2] however, because HCl–H$_2$O$_2$ mixtures tend to form flow-blocking bubbles within the Ln-Spec resin. This problem is avoided by loading in HNO$_3$–H$_2$O$_2$ as done by Wimpenny et al.[3] in their procedure for isolating Lu and Hf from Fe-free matrices.

(3) Improving the separation between Hf and Zr

For TIMS measurements of Hf isotope ratios, it was crucial to decrease the Zr/Hf to levels below ∼2 so that Hf would ionize efficiently.[1,6,10] During MC-ICP-MS analysis, even a high Zr/Hf value (natural ≈ 35) does not significantly inhibit the ionization of Hf.[8] Many analytical protocols therefore do not even attempt to separate these elements.[8,20–24] Indeed, zircon analyses by laser ablation (LA)-MC-ICP-MS will always be subject to natural Zr/Hf, but in that case, zircon grains are also used as isotopic

Fig. 3   Column dimensions.

standards and their mass bias behavior is likely similar to that of the unknowns. The standards are thus matrix-matched to the samples. This is not always the case for solution-based MC-ICP-MS, where a Zr-free Hf solution (*e.g.*, JMC-475) is used as a standard. Peters et al.[12] reported that at a Zr/Hf above 10 there is an observable bias on $^{176}Hf/^{177}Hf$ when using X skimmer- and Jet sample cones on a Thermo Scientific Neptune MC-ICP-MS. We have also periodically observed up to 3 ε-unit positive shifts in $^{176}Hf/^{177}Hf$ in a specific Hf cut that had a Zr/Hf of ∼7.2. At the same time, the $^{175}Lu/^{176}\Sigma$ monitor was elevated independent of the actual amount of Lu in the Hf fraction. Other samples having lower Zr/Hf showed no such shifts during the same analysis sessions. However, re-measurement of the high-Zr/Hf sample solution during later analysis sessions showed no shifts, and tests using an AMES Hf standard doped with AMES Zr also showed no shifts: The $^{176}Hf/^{177}Hf$ of 20 ppb AMES Hf solutions reproduced within 30 ppm for Zr/Hf up to 10, and no significant correlation between $^{176}Hf/^{177}Hf$ and Zr/Hf was observed. It seems that observed shifts for the high-Zr/Hf solutions are intermittent and related to the specific conditions affecting some analysis sessions where X- and Jet cones are used. It is also unclear whether Zr is the cause of these shifts. To eliminate the possibility of biases arising from high Zr/Hf, the separation of those two elements can be optimized by carefully adjusting the HF molarity of the HNO$_3$–HF mixture used to elute Zr. In addition, a high-Zr/Hf standard can be measured at the start of an analysis session to ensure that Hf isotope ratio measurements are insensitive to Zr.

(4) Avoiding ascorbic acid in eluted fractions to be used for Rb, Sr, Sm, and Nd analyses

In the procedure of Münker et al.,[2] the sample is loaded onto Ln-Spec resin in 3 M HCl—0.1 M ascorbic acid. The latter is used to avoid Fe in the Lu and Hf fractions by reducing Fe^{3+} to Fe^{2+}, which is not adsorbed strongly by the Ln-Spec resin and is eluted with the bulk matrix. This matrix fraction, which also contains Rb, Sr, Sm, and Nd is eluted in the first 20 ml of 3 M HCl[2] (including the loading volume and its ascorbic acid). However, drying down ascorbic acid-bearing solutions on a hot plate results in tarry residues that are difficult to re-dissolve for loading onto the next stage of chemistry. This difficulty is avoided by employing the first-stage cation column mentioned above in which the HFSE are eluted before Fe, and the HREE are eluted afterwards.

(5) Minimizing procedural blanks

When scaling down the amount of sample analyzed, the procedural blanks need to be reduced simultaneously to keep blank contributions negligible or correctable. This is especially important for Lu–Hf geochronological studies on small amounts of handpicked, low-Hf minerals. Miniaturizing the cation column and making the Ti elution more efficient can reduce the amount of reagents used significantly over previous methods.
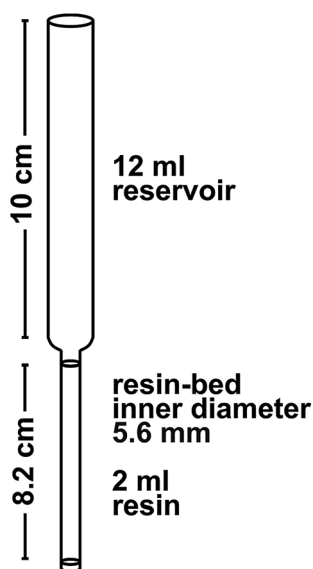
2326 | *J. Anal. At. Spectrom.*, 2015, **30**, 2323–2333

This journal is © The Royal Society of Chemistry 2015

Ion-exchange chromatography

The 2-stage ion-exchange chromatography for Lu–Hf geochronology that is presented in detail below meets all the aforementioned requirements and works reliably for small samples but also up to 100 mg of digested whole-rock powder. The first-stage cation column allows the direct separation of Rb, Sr, and Sm + Nd fractions if needed. The HFSE (including Hf) and the HREE (including Lu) are completely separated from each other, eliminating potential interferences. The HREE cut can be used without further processing for Lu ID analysis, whereas the Hf fraction needs further purification. As a second stage, an Ln-Spec column adapted from Münker et al.[2] and Wimpenny et al.[3] is used to isolate Hf from Ti and Zr, typically resulting in Zr/Hf < 1 after a single pass through the column. Compared to the Lu–Hf separation method previously used in our laboratory,[2] this optimized procedure yields cleaner Hf cuts while minimizing sample handling and the amount of acid consumed, and lowering the analytical blank to <10 pg.

Materials and reagents

The ion-exchange chromatography is performed in a class 100 laminar flow hood in a class 10 000 clean room environment. All columns are made from Kynar heat-shrink tubing (12.7–6.4 mm diameter; from Angst and Pfister) with the dimensions given in Fig. 3. Frits are cut from a 1.6 mm thick Thomapor® sintered plate made out of porous high-density polyethylene (HDPE, pore size 35 μm, from Reichelt Chemietechnik). All reagents except for H_2O and H_2O_2 have been distilled once using a Savillex DST-1000 Acid Purification System and diluted with 18.2 MΩ cm H_2O (Millipore Milli-Q®, hereafter "MQ").

Sample digestion

Up to 100 mg of whole-rock powder, or mineral grains (we tested garnet and apatite) are weighed into 15 ml Savillex Teflon® vials and covered with MQ H_2O. Mixed spikes enriched in ^{176}Lu–^{180}Hf, ^{149}Sm–^{150}Nd, and ^{87}Rb–^{84}Sr are added before digesting the samples with concentrated HF–HNO_3 (2 : 1) in capped vials on a hot plate at 120 °C. After 24–48 h, the vials are opened and the acids evaporated (such hot plate digestions are insufficient for the full digestion of zircon-bearing rocks. For such samples, other methods can be used, e.g., digestions in high-pressure autoclaves). Apatite is dissolved in 3 ml 6 M HCl—0.06 M HF instead of HF–HNO_3. After decomposition, all samples are dried down with 1 ml of 15 M HNO_3 three times to break down fluorides before being converted to chlorides by drying down with 1–5 ml of 10 M HCl.

Column I

The initial cation column is a miniaturized version of Patchett and Tatsumoto's column A[1]. It is filled with 2 ml of Bio-rad AG® 50W-X8 resin (200–400 mesh), which has an operating capacity of 2–3 meq. The resin is cleaned with 3–4 reservoir volumes (RV, ≈12 ml) of 6 M HCl and 1 RV of 2 M HF (Table 2). Between these

two steps, the columns are backwashed with MQ H_2O to prevent expulsion of the frit by resin expansion. For the cation-exchange chromatography, samples up to 50 mg are taken up in 170 μl 6 M HCl at 140 °C on a hot plate. Once the sample is completely dissolved, it is sequentially diluted with 780 μl H_2O and then 50 μl 2 M HF to 1 M HCl—0.1 M HF, transferred to a test tube and centrifuged. (For larger sample sizes, the loading volume is scaled up accordingly, which may broaden the Rb and Sr peaks but does not influence the HFSE and REE elution.) Clear sample solutions are then pipetted onto the columns, leaving any undigested grains (e.g., refractory zircon and rutile inclusions from garnet) behind. The HFSE (including Hf) are eluted immediately and need to be collected already during loading. Following the elution scheme summarized in Table 2, the sample matrix rinses off first in 1.5 M HCl, followed by Rb and Sr. The Rb fraction can be analyzed using the method of e.g., Nebel et al.,[25,26] whereas Sr generally requires further purification, for example using traditional cation exchange[27] or a Sr-Spec column.[28] Lutetium and other HREE are collected in 8 ml of 2.5 M HCl. After evaporating to dryness on a hot plate at 120 °C, this fraction is treated with 200 μl of 0.1 M HNO_3—4% H_2O_2 and dried down at 80 °C to oxidize any organic residues from the resin and reagents. After redissolving in 0.1 M HNO_3,

Table 2 Elution schemes for the two-stage Lu–Hf ion exchange chromatography[a]

Step	Acid
Column I: 2 ml AG 50W-X8 (200-400 mesh)	
Preparation	1 RV 6 M HCl
	2 × backwash with MQ H_2O
	1 RV 2 M HF
	2 RV 6 M HCl
	2 × backwash with MQ H_2O
Condition	2 ml 1 M HCl—0.1 M HF
Load sample, collect HFSE (Hf)	1–2 ml 1 M HCl—0.1 M HF
Collect HFSE (Hf)	0.5 ml 1 M HCl—0.1 M HF
Collect HFSE (Hf)	2 ml 1 M HCl—0.1 M HF
Elute matrix	4 ml 1.5 M HCl
Collect Rb	4 ml 1.5 M HCl
Rinse	10 ml 1.5 M HCl
Collect Sr	8 ml 1.5 M HCl
Rinse	8 ml 1.5 M HCl
Collect HREE (Lu)	8 ml 2.5 M HCl
Collect LREE (Sm, Nd)	6 ml 6 M HCl
Column II: 2 ml Ln-Spec resin (100–150 μm)	
Preparation	1 RV 6 M HCl
	1 RV 2 M HF
	1 RV 6 M HCl
	1 RV 2 M HF
	2 ml MQ H_2O
Condition	2 × 2 ml 3 M HNO_3—1% H_2O_2
Load HFSE cut from column I	2 ml 3 M HNO_3—1% H_2O_2
Elute Ti	4–6 × 2 ml 3 M HNO_3—1% H_2O_2
Wash off H_2O_2	2 ml 0.1 M HNO_3
Elute Zr	6 × 4 ml 0.5 M HNO_3—0.06 M HF
Collect Hf	3 ml 0.56 M HNO_3—0.3 M HF

[a] RV: reservoir volume (≈12 ml).

Table 3 Faraday cup and resistor configurations for high precision Hf isotope and Lu ID analysis

Cup	L4	L3	L2	L1	C	H1	H2	H3	H4
High-concentration Hf analysis									
Isotope	^{173}Yb	^{175}Lu	^{176}Hf	^{177}Hf	^{178}Hf	^{179}Hf	^{180}Hf	^{181}Ta	^{183}W
Resistor (Ω)	10^{12}	10^{12}	10^{11}	10^{11}	10^{11}	10^{11}	10^{10}	10^{11}	10^{11}
Low-concentration Hf analysis									
Isotope	^{173}Yb	^{175}Lu	^{176}Hf	^{177}Hf	^{178}Hf	^{179}Hf	^{180}Hf	^{181}Ta	^{183}W
Resistor (Ω)	10^{11}	10^{12}	10^{12}	10^{12}	10^{11}	10^{11}	10^{11}	10^{11}	10^{11}
Lu ID analysis									
Isotope	^{166}Er	^{167}Er	^{171}Yb	^{172}Yb	^{173}Yb	^{174}Yb	^{175}Lu	^{176}Lu	^{178}Hf
Resistor (Ω)	10^{11}	10^{11}	10^{11}	10^{11}	10^{11}	10^{10}	10^{11}	10^{12}	10^{12}

the sample is ready for MC-ICP-MS analysis. The light rare earth elements (LREE) can also be eluted in 6 M HCl and dried down for further separation of Nd and Sm following the procedure of e.g., Richard et al.[29] or Pin and Zalduegui.[30]

Column II

Columns dedicated to Hf purification are filled with 2 ml of Eichrom Ln-Spec resin (100–150 μm) and cleaned with 6 M HCl and 2 M HF steps (Table 2). The dried HFSE cuts from column I are treated with 200 μl of 0.56 M HNO_3—0.3 M HF—4% H_2O_2 and dried gently at 80 °C to oxidize the organic contaminants derived from the resin and acids. If this step is omitted, the samples will not fully dissolve when taken up in 2 ml of 3 M HNO_3—1% H_2O_2 for loading. To prevent breakdown of the H_2O_2, this loading mixture should not be heated. Instead, complete sample dissolution can be achieved by placing capped vials into an ultrasonic bath for 30 minutes. The clear yellow sample solutions are then loaded onto pre-conditioned Ln-Spec columns.[3] Titanium is rinsed off with up to 12 ml 3 M HNO_3—1% H_2O_2 (adding 2 ml at a time) until the eluate is colorless. The remaining H_2O_2 is washed off the columns using 0.1 M HNO_3 before Zr is eluted with six 4 ml batches of 0.5 M HNO_3—0.06 M HF. The HF molarity needs to be exact to achieve Zr/Hf < 1. The purified Hf cuts are then collected in 3 ml of 0.56 M HNO_3—0.3 M HF, dried down and treated again with the oxidizing agent described above.

Column calibration analysis

The effectiveness of the chemical separation was tested using a Thermo Scientific XSeries II quadrupole ICP-MS at the Institut für Planetologie at WWU Münster. The eluted fractions were doped with 10 ng In, which was used as an internal standard and scanned for a broad range of major and trace elements (Na, Mg, Al, Si, P, K, Ca, Ti, V, Cr, Mn, Fe, Co, Ni, Rb, Sr, Sc, Y, Zr, Nb, Mo, In, Ba, REE, Hf, Ta, and W). The samples were analyzed using a Peltier-cooled cyclonic quartz glass spray chamber and an ESI Microflow PFA nebulizer. Sample solutions were introduced using a peristaltic pump at an uptake rate of ~670 μl min⁻¹, yielding a sensitivity of ~1300 kcps for a 10 ppb In solution. Signals were detected in standard resolution and

acquired by peak-jumping using a single channel per peak with a dwell time of 10 ms for each individual mass. One analysis consisted of three main runs with 50 measurements (sweeps) per run. Solution standards with known element concentrations were measured under the same conditions and used to calculate the element concentrations in each eluted fraction.

Isotope analysis

Hafnium

High precision Hf isotope analyses are performed on a Thermo Scientific Neptune Plus MC-ICP-MS at the Institut für Mineralogie at WWU Münster. The instrument is equipped with three 10^{12} Ω resistors, which allow a precise measurement of signals below 5×10^{-11} A. The main isotopes of Hf (^{176}Hf, ^{177}Hf, ^{178}Hf, ^{179}Hf, and ^{180}Hf) and one of each interfering element (^{173}Yb, ^{175}Lu, ^{181}Ta, and ^{183}W) are measured simultaneously using the Faraday cup configuration shown in Table 3. For high-concentration analyses (up to 40 ppb Hf), two of the sensitive resistors are used for the Yb and Lu interference monitors, whereas a 10^{10} Ω resistor is used for the spike isotope ^{180}Hf (or ^{181}Ta, whichever signal is generally higher). For low-concentration analyses (<10 ppb), however, the 10^{12} Ω resistors are used for measuring the ^{175}Lu, ^{176}Hf, and ^{177}Hf signals.

An Aridus II™ Desolvating Nebulizer System equipped with a Cetac C-Flow PFA concentric nebulizer with a flow rate of ~80 μl min⁻¹ is used as the sample introduction system. This setup produces particularly stable signals. An X-skimmer and Jet sample cone are installed to enhance the sensitivity up to 2000 V ppm⁻¹ for Hf, which corresponds to a signal of ≈0.35 V on ^{177}Hf for 1 ppb Hf solutions. An autosampler is used to maintain consistent time intervals for the wash out (5 min in 1 M HNO_3—0.6 M HF), on-peak zero measurements (4 min), and sample solution uptake (1 min before analysis). Baselines are measured at all masses without defocusing ("on-peak zeroes", OPZ) while drawing trace element-free 0.56 M HNO_3—0.3 M HF into the nebulizing system. Samples are dissolved in 0.5 ml of the same acid mixture and diluted to appropriate concentrations. The amounts of Hf and Zr (monitored on mass 90) in each sample are determined by manual peak-hopping on pre-dilutions (20 μl sample solution in 1 ml
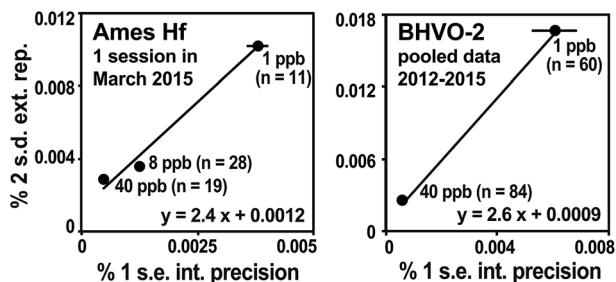
Fig. 4 The external reproducibility of $^{176}Hf/^{177}Hf$ is estimated from the relationship between the average internal analysis statistics (% 1 s.e. of 60 cycles) and the external reproducibility of replicate analyses (% 2 s.d. of multiple analyses) of the Münster AMES Hf standard (left) analyzed at different concentrations, following the method of Bizzarro et al.[36] The relationship holds e.g., for replicate analyses of BHVO-2 (right). The resulting trends are used to estimate the % 2 s.d. uncertainties for samples that can only be analyzed once. The slopes of the trends are typically in the range of 2.5 to 3.0.

acid). The samples are then diluted to the same Hf concentrations as the respective standard. Each analysis comprises one block of 60 integrations of 4.2 s each. An exponential mass bias correction is applied using $^{179}Hf/^{177}Hf = 0.7325$. Sample analyses are bracketed by analyses of the Münster AMES Hf solution (which is isotopically equivalent to JMC-475) and all values are normalized to a $^{176}Hf/^{177}Hf$ of 0.282160 for that standard.

Lutetium

The Lu concentrations were determined by isotope dilution (ID)-MC-ICP-MS on a Thermo Scientific Neptune Plus at the Institut für Mineralogie at WWU Münster. The utilized equipment and operating conditions are similar to those described above. Lutetium, which has only two naturally occurring isotopes (^{175}Lu and ^{176}Lu), is typically doped with a non-interfering element such as Er[31] or Re[2,32] for mass bias correction, or concomitantly eluted Yb may be used.[8,15,33,34] In the HREE fraction obtained from column I, natural Yb and Er are quantitatively recovered. Ytterbium creates an isobaric interference on ^{176}Lu that can be precisely corrected,[12,15,34] whereas Er has several stable, non-interfering isotopes that can be used for mass bias correction (e.g., $^{167}Er/^{166}Er = 0.6841$). Accordingly, all Lu- and Yb-standards used are doped with 5 ppb Er. Again, predilutions are used to determine the HREE concentrations of the samples, which are then diluted to 1–2 ppb Lu for analysis. The cup configuration given in Table 3 is used for acquisition, collecting 30 cycles with an integration time of 4.2 s.

Analytical uncertainties

Geochronological applications generally involve testing that the samples satisfy the isochron assumptions, namely that all samples had the same initial isotope composition, that they became closed systems simultaneously, and that they have remained closed systems. Samples meeting these criteria will define a linear trend on an isochron diagram whereby the observed scatter of points can be explained by the analytical uncertainties alone. Higher degrees of scatter—evidenced by

MSWD values significantly greater than the expected value of 1—indicate that at least one of the isochron assumptions has been violated.[35] Detecting such geologic scatter with MSWD values requires realistic assessments of the analytical uncertainties, which vary according to the amounts of daughter and parent elements available for measurement, as well as the degree of error magnification due to over- or under-spiking. For this reason, we recommend that the uncertainties on each isochron point be individually estimated rather than being assigned a "blanket" value.

The external reproducibility of $^{176}Hf/^{177}Hf$ is estimated for each data point on the basis of its internal measurement statistics as described by Bizzarro et al.[36] This method has previously been documented to yield realistic estimates for Hf isotope analyses.[13] Multiple analyses of the AMES Hf solution standard measured at different concentrations are used to establish the relationship between internal measurement uncertainty (% 1 s.e. of the 60 integrations) and external reproducibility (% 2 s.d. of $n \geq 5$ analyses; Fig. 4a). This trend is then used to transform the internal analytical uncertainty of samples that can only be measured once or twice into an estimated external uncertainty, i.e., 2 s.d. that would be expected if the sample were measured many times. In our laboratory, trend slopes are typically between 2.5 and 3.0. Repeated analyses of terrestrial reference rocks yield trends that agree with those of solution standards, indicating that the latter can be applied to rock samples that have been spiked and processed through chemistry (Fig. 4b). Any additional uncertainty on $^{176}Hf/^{177}Hf$ arising from the Lu interference corrections (equation above) is added quadratically to the 2 s.d. external reproducibility.

The analytical uncertainty of $^{176}Lu/^{177}Hf$ includes an error magnification that accounts for the effects of over- and under-spiking.[37] The error magnification factor F is calculated following the equation

$$F = R_M \left| \frac{R_N - R_S}{(R_N - R_M)(R_M - R_S)} \right|$$

in which R is the isotope ratio ($^{176}Lu/^{175}Lu$ or $^{180}Hf/^{177}Hf$) of the sample-spike mix (R_M), natural (R_N), and the spike (R_S).[38] The typical precisions of $^{176}Lu/^{175}Lu$ and $^{180}Hf/^{177}Hf$ for natural Lu and Hf standard solutions are 0.2% and 0.01%, respectively. These are multiplied by their respective error magnification factors (F) and then added quadratically to yield the uncertainty on $^{176}Lu/^{177}Hf$ in percent. More than 99% of this uncertainty originates from the isotope dilution analysis of Lu, which has only two isotopes and can therefore not be determined as precisely as Hf. The Hf contribution to the uncertainty on $^{176}Lu/^{177}Hf$ can be neglected.

Results and discussion

Efficiency of the chemical separation

Hafnium is eluted in 1 M HCl—0.1 M HF from the cation column together with Na, Mg, Al, Ti, Fe, Nb, Zr, Mo, Ta and W (Fig. 5). The REE are fully adsorbed to the cation resin in this acid, resulting in complete separation of Lu and Hf. Lutetium, Yb and Er are collected in 2.5 M HCl after eluting the major
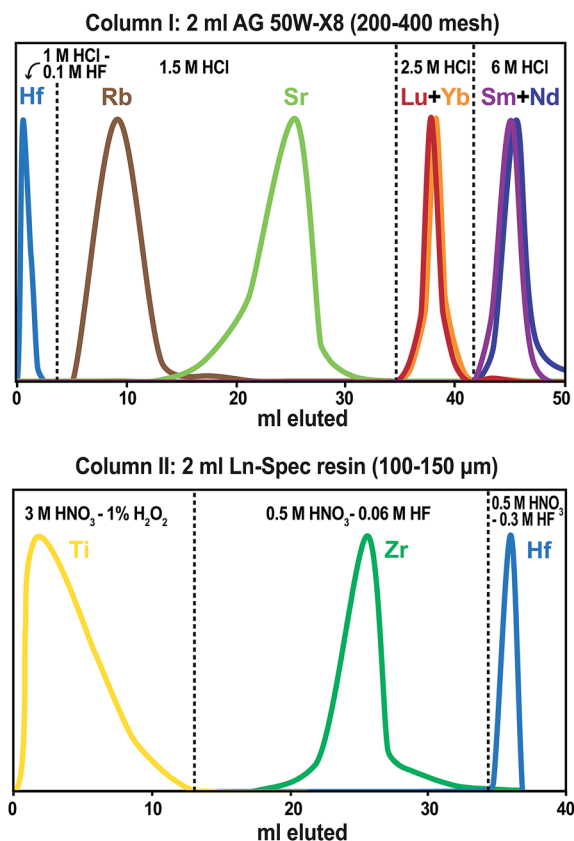
Column I: 2 ml AG 50W-X8 (200-400 mesh)

Column II: 2 ml Ln-Spec resin (100-150 µm)

Fig. 5 Elution curves for the described ion-exchange chromatography. The peak shapes have been normalized to the same maximum value. Top: column I (2 ml AG 50W-X8, 200−400 mesh), and bottom: column II (2 ml Ln-Spec resin, 100−150 µm).

elements and Rb and Sr in 1.5 M HCl. For up to 100 mg of whole-rock, phosphate, or garnet, no breakthrough of HREE was observed before switching from 1.5 M to 2.5 M HCl, even if the columns were left overnight or another 2 ml of 1.5 M HCl were added before collecting Lu.

In addition to Lu–Hf, fractions for Rb–Sr and Sm–Nd geochronology can also be collected from the cation column. A fraction containing 90% of the sample Rb, together with various amounts of Mg, K, Mn, Fe, Co, and Ni, is collected in 4 ml of 1.5 M HCl (Table 2, Fig. 5). Although the additional elements do not have isotopes that isobarically interfere with ^{85}Rb or ^{87}Rb, they may affect mass bias behavior during MC-ICP-MS analysis. This is not the case for thermal ionization mass spectrometry (TIMS), but an additional cleanup of the Rb fraction[25,26] is advisable for either measurement method. Only about 70–80% of the total Sr is collected to avoid large quantities of Ca, which is mostly eluted in between Rb and Sr. For high-Ta samples (such as BIR-1), we observed an elevated Ta/Sr of 0.3. For Sr isotope analyses by MC-ICP-MS or TIMS, the Sr fraction should be further purified.[27,28] The LREE, including Sm and Nd, are eluted in 6 M HCl and can also be separated further for geochronological applications.[29,30]

Hafnium is purified on an Ln-Spec column that never gets loaded with REE-bearing samples, which is important for keeping the ^{175}Lu/$^{176}\Sigma$ monitor below 0.0001. Titanium forms a

yellow to orange complex in 3 M HNO$_3$—1% H$_2$O$_2$, and is immediately eluted during loading.[3] Up to 12 ml of this acid mixture are added in 2 ml steps until the eluate is colorless, indicating that Ti has been almost quantitatively eluted from the column. Using this simple criterion, a sufficient separation of Ti and Hf is achieved, resulting in Ti/Hf < 0.1. Zirconium is rinsed off effectively with six 4 ml batches of 0.5 M HNO$_3$—0.06 M HF, whereas Hf remains on the column until the HF molarity is increased to 0.3 M. Separation techniques previously used at our laboratory[2] yielded Zr/Hf in the range of 2 to 15, whereas the method reported here consistently yields values <1. For up to 100 mg basalt, the total Hf recovery is typically 98% or more. Deliberate overloading of the initial cation column with 200 mg of digested BHVO-2 powder still produces a clean Hf fraction (^{175}Lu/$^{176}\Sigma$ monitor < 0.0001, Ti/Hf = 0.05, and Zr/Hf = 0.1) and a yield of 78%. Tests on 100–200 mg of garnet result in Hf yields of about 75%. For 100 mg garnet samples, the Hf is efficiently purified, whereas a 200 mg garnet sample resulted in an elevated Lu monitor (^{175}Lu/$^{176}\Sigma$) of 0.0017. This breakthrough of HREE indicates that the operating capacity of the cation resin is not sufficient for sample sizes above 3 meq. Such overloading of column I can be avoided by either dividing large sample loads among several first-stage columns or using a larger first-stage cation column.[1] Alternatively, a 1 ml Ln-Spec column[2] could also be used to separate the HFSE and HREE from the matrix before processing through cation column I. Special care should be taken to keep the Ln-Spec resin in column II REE-free. For phosphates, the Hf cuts are very clean with respect to other elements, but the Hf recovery is only in the range of 25 to 50 %, which is probably caused by Hf sequestration by precipitates that formed when the samples were dried down after the digestion. We therefore suggest dissolving phosphates in 6 M HCl and diluting this acid to molarities appropriate for direct loading onto the first column, *i.e.* 1 M HCl—0.1 M HF, without drying down in between.

Reference materials

The analytical procedure described in this study was tested on four different international reference rocks (BHVO-2, JB-1, BIR-1, and G-2). For comparison, each material was also processed once using the Münker *et al.*[2] method. Most samples were fully spiked before digestion for simultaneous IC and ID analysis, with the exception of two BHVO-2 aliquots ("E" and "F"), which were analyzed unspiked. Solution aliquots equivalent to *ca.* 50 mg digested whole-rock powder were typically loaded onto the columns. The 200 mg BHVO-2 fractions "D", "E" and "F" were split into aliquots after digestion and loaded onto four individual ion-exchange columns to test for possible variations in isotope composition induced by the chemical separation. No resolvable variations were observed.

For all individually processed digestions of the investigated reference materials, the Hf isotope compositions, as well as the Lu and Hf concentrations, are summarized in Fig. 6 and Table S1† in the online repository. Literature values[1,2,16,23,39–76] are given for comparison. For all materials investigated, the results for a total of 14 separate digestions of 50–200 mg powder
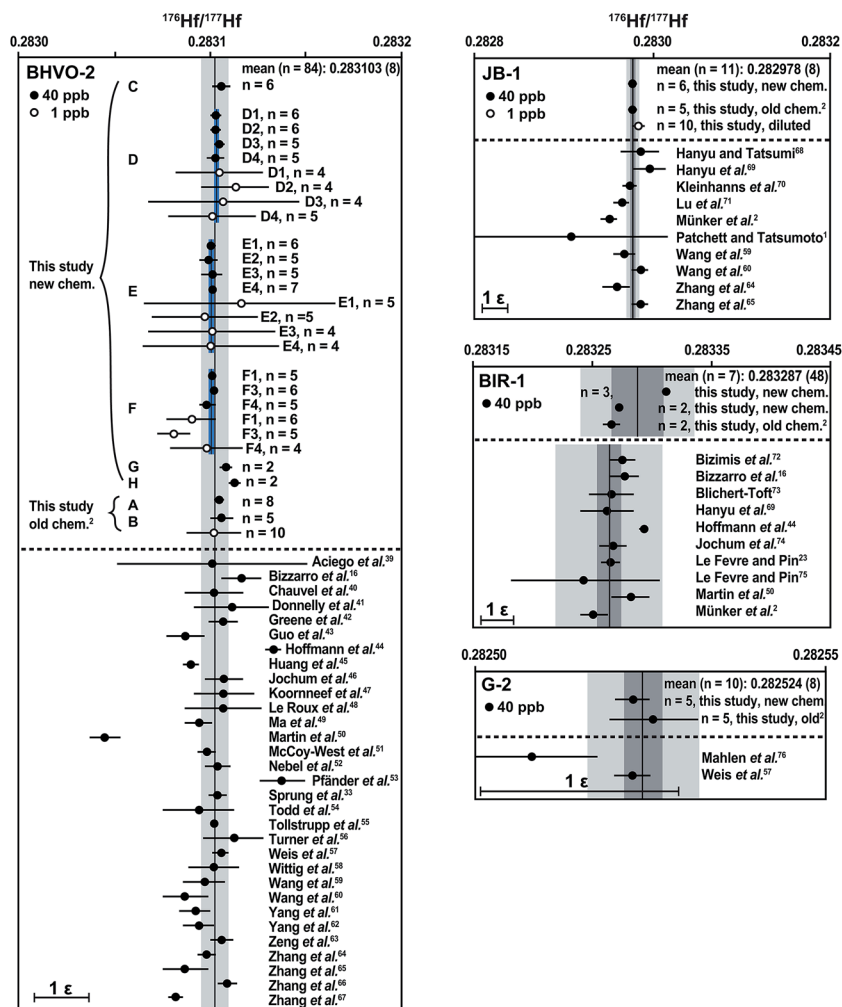
Fig. 6 Average Hf isotope composition for each individual digestion of the international reference rocks BHVO-2, JB-1, G-2 and BIR-1. Vertical black lines through the data represent the grand mean of all of our 40 ppb analyses with 95% confidence limits (dark grey bars). The 2 s.d. external reproducibility is shown with light grey bars and given in parentheses as uncertainties in the least significant digits. For BHVO-2, four aliquots of digestions D, E, and F were processed through four individual columns and measured separately. The average of the 40 ppb analyses for each digestion (D–F) is shown (short black lines) along with 95% confidence limits (blue bars). The scale bar on the lower left side of each diagram measures 1 ε-unit. All data have been normalized to a $^{176}Hf/^{177}Hf$ of 0.282160 for the JMC-475 Hf standard. For literature data, the quoted uncertainties on mean values were converted to 95% confidence limits when the number of measurements and type of uncertainty (s.e. vs. s.d.) could be ascertained. For n = 1–3, we converted 2 s.e. internal analysis statistics to 2 s.d. external reproducibility by multiplying by 2 assuming reproducibility behavior observed by Bizzaro et al.[36]

aliquots are in good agreement with the recommended values, independent of the separation procedure used. The following $^{176}Hf/^{177}Hf$ values are given with their 2 s.d. uncertainties in the least significant digits in parentheses. The average $^{176}Hf/^{177}Hf$ for all of our 40 ppb BHVO-2 analyses (eight digestions divided into 1–4 solution aliquots each) is 0.283103 (8), which is indistinguishable from the recommended value of $^{176}Hf/^{177}Hf$ = 0.283105 (11).[57] Two individual digestions of JB-1 processed through different separation techniques have an average $^{176}Hf/^{177}Hf$ of 0.282978 (8), whereas literature values range from 0.282951 (9)[2] to 0.282997 (18).[69] Three individual hot plate digestions of BIR-1 have $^{176}Hf/^{177}Hf$ values that vary from 0.283266 (15) to 0.283312 (3). Literature values range from 0.283244 (63)[75] to 0.283293 (4),[44] which overlaps with those of two of our digestions. The remaining digestion of BIR-1 yielded

a slightly higher $^{176}Hf/^{177}Hf$, which was reproduced in repeated analyses and is therefore most likely caused by sample heterogeneity (2 ε-unit variation for BIR-1). For G-2, two individual autoclave digestions were processed individually through different chemical separation methods, yielding an average $^{176}Hf/^{177}Hf$ of 0.282524 (8), which is indistinguishable from the recommended value of $^{176}Hf/^{177}Hf$ = 0.282522 (3).[57]

To test the instrument performance on small sample sizes, the Münster Ames Hf standard solution and several BHVO-2 Hf solutions ("B", "D", "E", and "F") were diluted to a concentration of 1 ppb (0.5 ng Hf per 0.5 ml solution per analysis). Repeated analyses of the 1 ppb BHVO-2 solutions yielded an average $^{176}Hf/^{177}Hf$ of 0.283101 (41), i.e., a precision of 1.5 ε-units. All individual 1 ppb analyses are within uncertainty of the mean of 40 ppb analyses and therefore accurate. In

This journal is © The Royal Society of Chemistry 2015

J. Anal. At. Spectrom., 2015, 30, 2323–2333 | 2331

upcoming tests, small sample aliquots (*e.g.*, 1 mg WR powder) will be digested and processed individually. The BHVO-2 reference material appears to be well suited for testing the accuracy of Hf isotope compositions measured on such small sample sizes because this recently formed basalt has a homogeneous Hf isotope composition.

Conclusions

Lutetium–hafnium geochronological studies require an efficient chemical separation to avoid subtle errors in $^{176}Hf/^{177}Hf$ and resulting isochron scatter caused by inaccurate corrections for the ^{176}Lu and ^{176}Yb interferences on ^{176}Hf. The ion-exchange method presented here lowers the HREE/Hf in the Hf fractions to insignificant levels, while also providing efficient removal of Ti and Zr, which may adversely affect the mass bias behavior of Hf during isotope analysis. The presented chromatography is thus especially well suited for Lu–Hf geochronology on high-Lu/Hf phases. Low procedural blanks are possible because of the reduced amount of acids required. These improvements over previous techniques, coupled with the use of sensitive 10^{12} Ω resistors during isotope ratio measurement by MC-ICP-MS, allow the use of Lu–Hf chronology for demanding applications where only ng quantities of Hf are available, *e.g.*, dating of small amounts of phosphate minerals,[34,77–81] single garnet grains, or even individual garnet growth-zones sampled by micro milling.[82] Furthermore, the employment of a first-stage cation column simplifies the application of multiple radioisotope systems (Lu–Hf, Sm–Nd, and Rb–Sr) to the same sample aliquot.

Acknowledgements

References

1 P. J. Patchett and M. Tatsumoto, *Contrib. Mineral. Petrol.*, 1980, **75**, 263–267.

2 C. Münker, S. Weyer, E. E. Scherer and K. Mezger, *Geochem., Geophys., Geosyst.*, 2001, **2**, DOI: 10.1029/2001gc000183.

3 J. B. Wimpenny, Y. Amelin and Q.-Z. Yin, *Anal. Chem.*, 2013, **85**, 11258–11264.

4 D. Herwartz, T. J. Nagel, C. Münker, E. E. Scherer and N. Froitzheim, *Nat. Geosci.*, 2011, **4**, 178–183.

5 R. Bast, E. E. Scherer, K. Mezger, M. Fischer-Gödde and P. Sprung, *Mineral. Mag.*, 2013, **77**, 665.

6 V. J. M. Salters and S. R. Hart, *Earth Planet. Sci. Lett.*, 1991, **104**, 364–380.

7 K. M. Barovich, B. L. Beard, J. B. Cappel, C. M. Johnson, T. K. Kyser and B. E. Morgan, *Chem. Geol.*, 1995, **121**, 303–308.

8 J. Blichert-Toft, C. Chauvel and F. Albarède, *Contrib. Mineral. Petrol.*, 1997, **127**, 248–260.

9 E. E. Scherer, K. L. Cameron, C. M. Johnson, B. L. Beard, K. M. Barovich and K. D. Collerson, *Chem. Geol.*, 1997, **142**, 63–78.

10 V. J. M. Salters, *Anal. Chem.*, 1994, **66**, 4186–4189.

11 S. C. Weyer, C. Münker, M. Rehkämper and K. Mezger, *Chem. Geol.*, 2002, **187**, 295–313.

12 S. T. M. Peters, C. Münker, F. Wombacher and B.-M. Elfers, *Chem. Geol.*, 2015, **413**, 132–145.

13 P. Sprung, E. E. Scherer, D. Upadhyay, I. Leya and K. Mezger, *Earth Planet. Sci. Lett.*, 2010, **295**, 1–11.

14 J. D. Vervoort, P. J. Patchett, U. Söderlund and M. Baker, *Geochem., Geophys., Geosyst.*, 2004, **5**, DOI: 10.1029/2004gc000721.

15 J. Blichert-Toft, M. Boyet, P. Télouk and F. Albarède, *Earth Planet. Sci. Lett.*, 2002, **204**, 167–181.

16 M. Bizzarro, J. A. Baker and D. Ulfbeck, *Geostand. Newsl.*, 2003, **27**, 133–145.

17 A. Bouvier, J. D. Verwoort and P. J. Patchett, *Earth Planet. Sci. Lett.*, 2008, **273**, 48–57.

18 J. N. Connelly, M. Bizzarro, A. N. Krot, A. Nordlund, D. Wielandt and M. A. Ivanova, *Science*, 2012, **338**, 651–655.

19 M. Bizimis, V. J. M. Salters and J. B. Dawson, *Contrib. Mineral. Petrol.*, 2003, **145**, 281–300.

20 N.-C. Chu, R. N. Taylor, V. Chavagnac, R. W. Nesbitt, R. M. Boella, J. A. Milton, C. R. German, G. Bayon and K. Burton, *Anal. At. Spectrom.*, 2002, **17**, 1567–1574.

21 J. N. Connelly, D. G. Ulfbeck, K. Thrane, M. Bizzarro and T. Housh, *Chem. Geol.*, 2006, **233**, 126–136.

22 K. David, J. L. Birck, P. Telouk and C. J. Allègre, *Chem. Geol.*, 1999, **157**, 1–12.

23 B. le Fèvre and C. Pin, *Anal. Chem.*, 2001, **73**, 2453–2460.

24 Y. H. Yang, H. F. Zhang, Z. Y. Chu, L. W. Xie and F. Y. Wu, *Int. J. Mass Spectrom.*, 2010, **290**, 120–126.

25 O. Nebel, K. Mezger, E. E. Scherer and C. Münker, *Int. J. Mass Spectrom.*, 2005, **246**, 10–18.

26 O. Nebel, E. E. Scherer and K. Mezger, *Earth Planet. Sci. Lett.*, 2011, **301**, 1–8.

27 S. R. Hart and C. Brooks, *Geochim. Cosmochim. Acta*, 1974, **38**, 1799–1806.

28 E. P. Horwitz, R. Chiarizia and M. L. Dietz, *Solvent Extr. Ion Exch.*, 1992, **10**, 313–336.

29 P. Richard, N. Shimizu and C. J. Allégre, *Earth Planet. Sci. Lett.*, 1976, **31**, 269–278.

30 C. Pin and J. F. S. Zaldueguí, *Anal. Chim. Acta*, 1997, **339**, 79–89.

31 T. J. Lapen, N. J. Mahlen, C. M. Johnson and B. L. Beard, *Geochem., Geophys., Geosyst.*, 2004, **5**, DOI: 10.1029/2003gc000582.

32 E. E. Scherer, C. Münker and K. Mezger, *Science*, 2001, **293**, 683–687.

33 P. Sprung, T. Kleine and E. E. Scherer, *Earth Planet. Sci. Lett.*, 2013, **380**, 77–87.

34 G. H. Barfod, O. Otera and F. Albarède, *Chem. Geol.*, 2003, **200**, 241–253.

35 I. Wendt and C. Carl, *Chem. Geol.*, 1991, **86**, 275–285.

2332 | *J. Anal. At. Spectrom.*, 2015, **30**, 2323–2333

This journal is © The Royal Society of Chemistry 2015

36 M. Bizzarro, J. A. Baker, H. Haack, D. Ulfbeck and M. Rosing, *Nature*, 2003, **421**, 931–933.

37 A. Stracke, E. E. Scherer and B. C. Reynolds, *Treatise on Geochemistry*, 2nd edn, 2014, pp. 71–86.

38 R. K. Webster, in *Methods in geochemistry*, ed. A. A. Smales and L. R. Wager, Interscience Publishers, New York, 1960, pp. 202–246.

39 S. M. Aciego, B. Bourdon, M. Lupker and J. Rickli, *Chem. Geol.*, 2009, **266**, 194–204.

40 C. Chauvel, S. Bureau and C. Poggi, *Geostand. Geoanal. Res.*, 2011, **35**, 125–143.

41 C. L. Donnelly, W. L. Griffin, S. Y. O'Reilly, N. J. Pearson and S. R. Shee, *Contrib. Mineral. Petrol.*, 2011, **161**, 351–371.

42 A. R. Greene, J. S. Scoates and D. Weis, *Geochem., Geophys., Geosyst.*, 2008, **9**, DOI: 10.1029/2008gc002092.

43 J. Guo, F. Guo, C. Y. Wang and C. Li, *Lithos*, 2013, **170–171**, 1–16.

44 J. E. Hoffmann, C. Münker, A. Polat, M. T. Rosing and T. Schulz, *Geochim. Cosmochim. Acta*, 2011, **75**, 6610–6628.

45 X.-L. Huang, Y. Niu, Y.-G. Xu, J.-L. Ma, H.-N. Qiu and J.-W. Zhong, *Contrib. Mineral. Petrol.*, 2013, **165**, 437–455.

46 K. P. Jochum, S. A. Wilson, W. Abouchami, M. Amini, J. Chmeleff, A. Eisenhauer, E. Hegner, L. M. Iaccheri, B. Kieffer, J. Krause, W. F. McDonough, R. Mertz-Kraus, I. Raczek, R. L. Rudnick, D. Scholz, G. Steinhoefel, B. Stoll, A. Stracke, S. Tonarini, D. Weis, U. Weis and J. D. Woodhead, *Geostand. Geoanal. Res.*, 2011, **35**, 193–226.

47 J. M. Koornneef, A. Stracke, B. Bourdon, M. A. Meier, K. P. Jochum, B. Stoll and K. Grönvold, *J. Petrol.*, 2012, **53**, 127–157.

48 V. le Roux, J.-L. Bodinier, O. Alard, S. Y. O'Reilly and W. L. Griffin, *Earth Planet. Sci. Lett.*, 2009, **279**, 76–85.

49 J. Ma, G. Wei, Y. Xu and W. Long, *Chem. Geol.*, 2010, **269**, 376–385.

50 C. Martin, S. Duchêne, B. Luais, P. Goncalves, E. Deloule and C. Fournier, *Contrib. Mineral. Petrol.*, 2010, **159**, 437–458.

51 A. J. McCoy-West, J. A. Baker, K. Faure and R. Wysoczanski, *J. Petrol.*, 2010, **51**, 2003–2045.

52 O. Nebel, M. L. A. Morel and P. Z. Vroon, *Geostand. Geoanal. Res.*, 2009, **33**, 487–499.

53 J. A. Pfänder, C. Münker, A. Stracke and K. Mezger, *Earth Planet. Sci. Lett.*, 2007, **254**, 158–172.

54 E. Todd, J. B. Gill, R. J. Wysoczanski, J. Hergt, I. C. Wright, M. I. Leybourne and N. Mortimer, *Geochem., Geophys., Geosyst.*, 2011, **12**, DOI: 10.1029/2011gc003683.

55 D. Tollstrup, J. Gill, A. Kent, D. Prinkey, R. Williams, Y. Tamura and O. Ishizuka, *Geochem., Geophys., Geosyst.*, 2010, **11**, DOI: 10.1029/2009gc002847.

56 S. Turner, M. Handler, I. Bindeman and K. Suzuki, *Chem. Geol.*, 2009, **266**, 187–193.

57 D. Weis, B. Kieffer, D. Hanano, I. Nobre Silva, J. Barling, W. Pretorius, C. Maerschalk and N. Mattielli, *Geochem., Geophys., Geosyst.*, 2007, **8**, DOI: 10.1029/2006gc001473.

58 N. Wittig, J. A. Baker and H. Downes, *Geochim. Cosmochim. Acta*, 2007, **71**, 1290–1311.

59 X.-C. Wang, Z.-X. Li, X.-H. Li, Q.-L. Li and Q.-R. Zhang, *Lithos*, 2011, **127**, 427–440.

60 Y. Wang, Z.-F. Zhao, Y.-F. Zheng and J.-J. Zhang, *Lithos*, 2011, **125**, 940–955.

61 Y.-H. Yang, F.-Y. Wu, S. A. Wilde, X.-M. Liu, Y.-B. Zhang, L.-W. Xie and J.-H. Yang, *Chem. Geol.*, 2009, **264**, 24–42.

62 Y. H. Yang, F.-Y. Wu, S. A. Wilde and L.-W. Xie, *Int. J. Mass Spectrom.*, 2011, **1**, 47–52.

63 G. Zeng, L.-H. Chen, S.-L. Hu, X.-S. Xu and L.-F. Yang, *Geochem., Geophys., Geosyst.*, 2013, **14**, DOI: 10.1002/ggge.20127.

64 L.-C. Zhang, X.-H. Zhou, J.-F. Ying, F. Wang, F. Guo, B. Wan and Z.-G. C. Zhang, *Chem. Geol.*, 2008, **256**, 12–23.

65 J.-J. Zhang, Y.-F. Zheng and Z.-F. Zhao, *Lithos*, 2009, **110**, 305–326.

66 Y.-L. Zhang, C.-Z. Liu, W.-C. Ge, F.-Y. Wu and Z.-Y. Chu, *Lithos*, 2011, **126**, 233–247.

67 G.-L. Zhang, L.-H. Chen and S.-Z. Li, *Earth Planet. Sci. Lett.*, 2013, **383**, 153–163.

68 T. Hanyu and Y. Tatsumi, *Geophys. Res. Lett.*, 2002, **29**, DOI: 10.1029/2002gl015856.

69 T. Hanyu, S. Nakai and R. Tatsuta, *Geochem. J.*, 2005, **39**, 83–90.

70 I. C. Kleinhanns, K. Kreissig, B. S. Kamber, T. Meisel, T. F. Nägler and J. D. Kramers, *Anal. Chem.*, 2002, **74**, 67–73.

71 Y. Lu, A. Makishima and E. Nakamura, *J. Anal. At. Spectrom.*, 2007, **22**, 69–76.

72 M. Bizimis, G. Sen, V. J. M. Salters and S. Keshav, *Geochim. Cosmochim. Acta*, 2005, **69**, 2629–2646.

73 J. Blichert-Toft, *Geostand. Newsl.*, 2001, **25**, 41–56.

74 K. P. Jochum, B. Stoll, K. Herwig, M. Willbold, A. W. Hofmann, M. Amini, S. Aarburg, W. Abouchami, E. Hellebrand, B. Mocek, I. Raczek, A. Stracke, O. Alard, C. Bouman, S. Becker, M. Dücking, H. Brätz, R. Klemd, D. de Bruin, D. Canil, D. Cornell, C.-J. de Hoog, C. Dalpé, L. Danyushevsky, A. Eisenhauer, Y. Gao, J. E. Snow, N. Groschopf, D. Günther, C. Latkoczy, M. Guillong, E. H. Hauri, H. E. Höfer, Y. Lahaye, K. Horz, D. E. Jacob, S. A. Kasemann, A. J. R. Kent, T. Ludwig, T. Zack, P. R. D. Mason, A. Meixner, M. Rosner, K. Misawa, B. P. Nash, J. Pfänder, W. R. Premo, W. D. Sun, M. Tiepolo, R. Vannucci, T. Vennemann, D. Wayne and J. D. Woodhead, *Geochem., Geophys., Geosyst.*, 2006, **7**, DOI: 10.1029/2005gc001060.

75 B. le Fèvre and C. Pin, *Anal. Chim. Acta*, 2005, **543**, 209–221.

76 N. J. Mahlen, B. L. Beard, C. M. Johnson and T. J. Lapen, *Geochem., Geophys., Geosyst.*, 2008, **9**, DOI: 10.1029/2007gc001605.

77 E. Scherer, C. Münker and K. Mezger, *Science*, 2001, **293**, 683–687.

78 U. Söderlund, P. J. Patchett, J. D. Vervoort and C. E. Isachsen, *Earth Planet. Sci. Lett.*, 2004, **219**, 311–324.

79 Y. Amelin, *Science*, 2005, **310**, 839–841.

80 G. H. Barfod, E. J. Krogstad, R. Frei and F. Albarède, *Geochim. Cosmochim. Acta*, 2005, **69**, 1847–1859.

81 D. Larsson and U. Söderlund, *Chem. Geol.*, 2005, **224**, 201–211.

82 A. D. Pollington and E. F. Baxter, *Chem. Geol.*, 2011, **281**, 270–282.